



Remote Sensing Laboratory
Dept. of Information Engineering and Computer Science
University of Trento
Via Sommarive, 9, I-38123 Povo, Trento, Italy



A Wavelet Temporal Analysis of Polarimetric Decomposition Parameters over Alpine Glaciers

D. Pirrone
A. M. Atto
E. Trouvé

Annecy-Le-Vieux, June 11, 2019

Outline

1

Introduction

2

Aim of the Work

3

Temporal Wavelet Framework for PolSAR Image Time Series

4

Case Study: Evolution of the Argentière Glacier

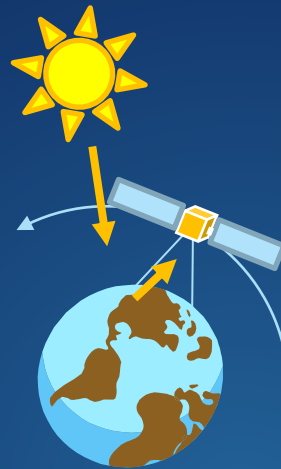
5

Conclusions and Future Developments

Imaging with Synthetic Aperture Radar

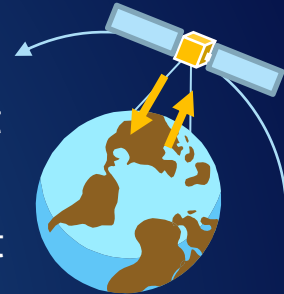
Passive optical sensors:

- ✓ For useful data, the two scenes should have:
 - Sunlight condition;
 - Clouds absence.
- ✓ “Human-friendly” images.

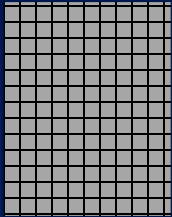


Microwave active sensors:

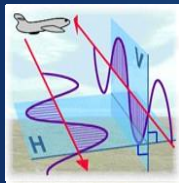
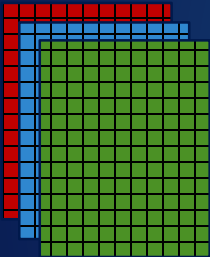
- ✓ Acquisitions are independent from sunlight and weather conditions.
- ✓ Image interpretation is not straightforward.



Information Enhancement in SAR imagery



- ✓ A large part of SAR imagery presents spatial resolution of decades of meters and a single polarimetric channel.
- ✓ This information has been largely exploited in the literature.
- ✓ The **recent technological trend** has moved to the acquisition of data with more polarimetric channels.



Polarimetric SAR (PolSAR) imagery

- Two (i.e., **dual-pol**) or four (i.e., **full-pol**) polarimetric channels;
- Polarimetric scattering **discriminate larger number of targets**.



Single-pol SAR image of Los Angeles (HH)



Full-pol SAR Pauli RGB image of Los Angeles
(R: HH-VV; G: HV; B: HH+VV)

Motivation

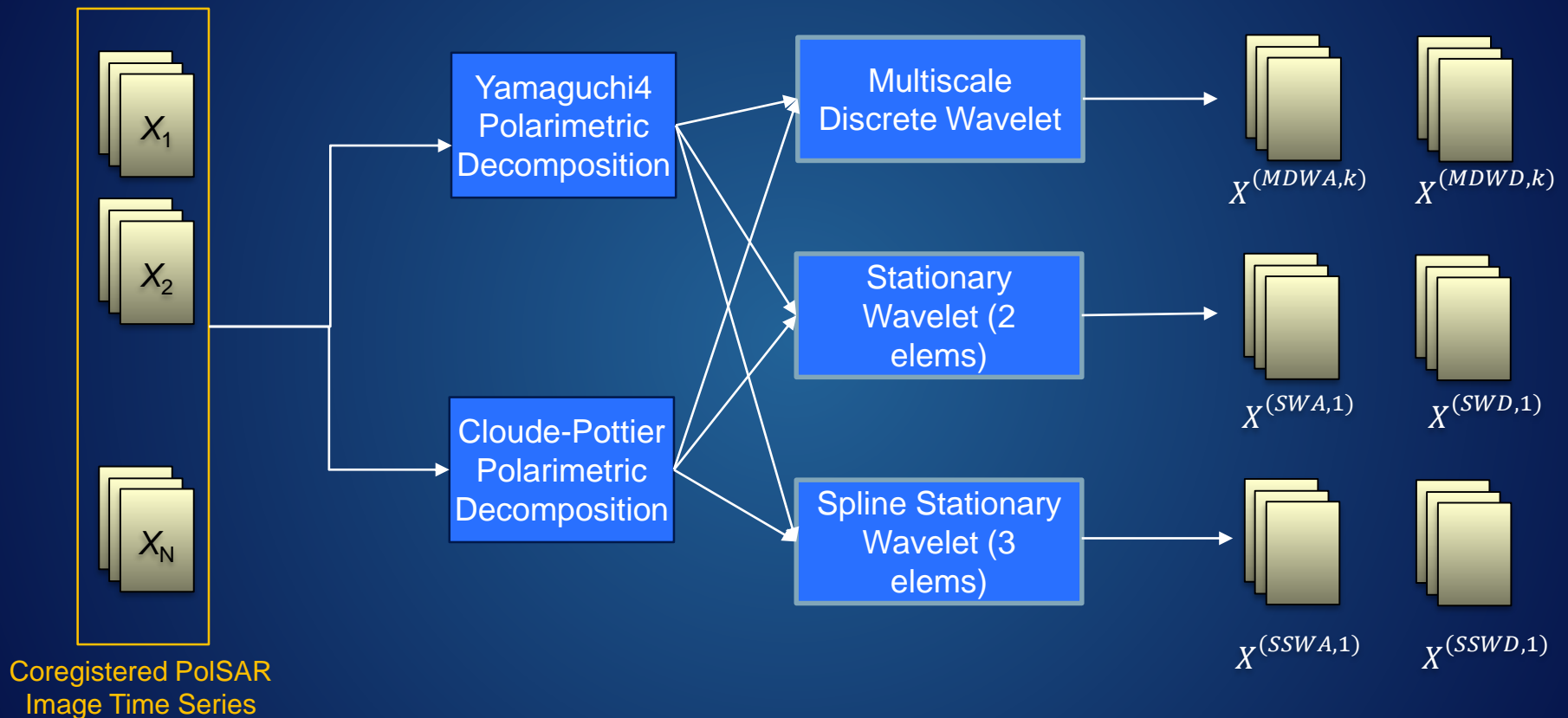
- ✓ The continuous acquisition of dual- and full-polarimetric SAR images open novel opportunities for exploiting image time series for monitoring applications.
- ✓ The literature proposed some methodologies for exploiting single-pol SAR image time series for multi-temporal CD analysis.
- ✓ The polarimetric multi-temporal information has been mainly exploited for the analysis of temporal trend of features in specific applications (e.g., snow monitoring or crop monitoring).

Open issue: the use of full-polarimetric information in image time series has been poorly exploited for detecting changes with different evolution.

Aim of the contribution

- ✓ The proposed contribution aims at defining a joint arithmetic-geometric wavelet **framework for the analysis of full-polarimetric image time series**.
- ✓ The framework includes:
 - The **selection of polarimetric decomposition features** carrying the relevant scattering information of the targets.
 - The **selection of wavelet transforms** relevant for the **sparse representation** of the **multi-temporal decomposition features**.
- ✓ The information in the framework both:
 - **Separates natural classes** based on their **multi-temporal content**.
 - Detectes **multi-temporal changes** and characterize **their evolution**.
- ✓ **The contribution will test** the proposed framework on **real multitemporal PolSAR dataset** acquired from Radarsat-2 mission over the Argentière glacier.

Proposed approach



Polarimetric Scattering Information

- ✓ Scattering information can be represented with the **Pauli** scattering vector k_p .
- ✓ **Three main mechanisms associated:**
 - Double bounce (HH-VV)
 - Volume scattering (HH+VV)
 - Surface scattering (HV)
- ✓ Distributed targets are represented with average scattering information of **Coherency matrix T** or its **polarimetric decompositions**.
- ✓ **Yamaguchi4 decomposition (Y4D)** considers the scattering combination of different mechanisms [1].

$$k_p = 1/\sqrt{2} [S_{hh} + S_{vv}, S_{hh} - S_{vv}, 2S_{hv}]$$

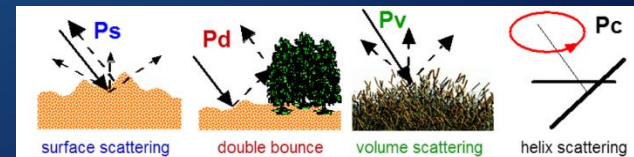


$$T = \langle k_p, k_p \rangle = \begin{bmatrix} T_{11} & T_{12} & T_{13} \\ T_{21} & T_{22} & T_{23} \\ T_{31} & T_{32} & T_{33} \end{bmatrix}$$

Coefficients for scattering power

$$T = f_s T_s + f_d T_d + f_v T_v + f_c T_c$$

Coherency associated to elementary targets



[1] Yamaguchi, Y., et al. "Four-component Scattering Power Decomposition with Rotation of Coherency Matrix." *IEEE Transactions on Geoscience and Remote Sensing* 49.6 (2011): 2251-2258.

Eigen-based Decomposition

✓ Cloude-Pottier decomposition (CPD) is applied on T , obtaining eigenvectors v_i and eigenvalues λ_i .

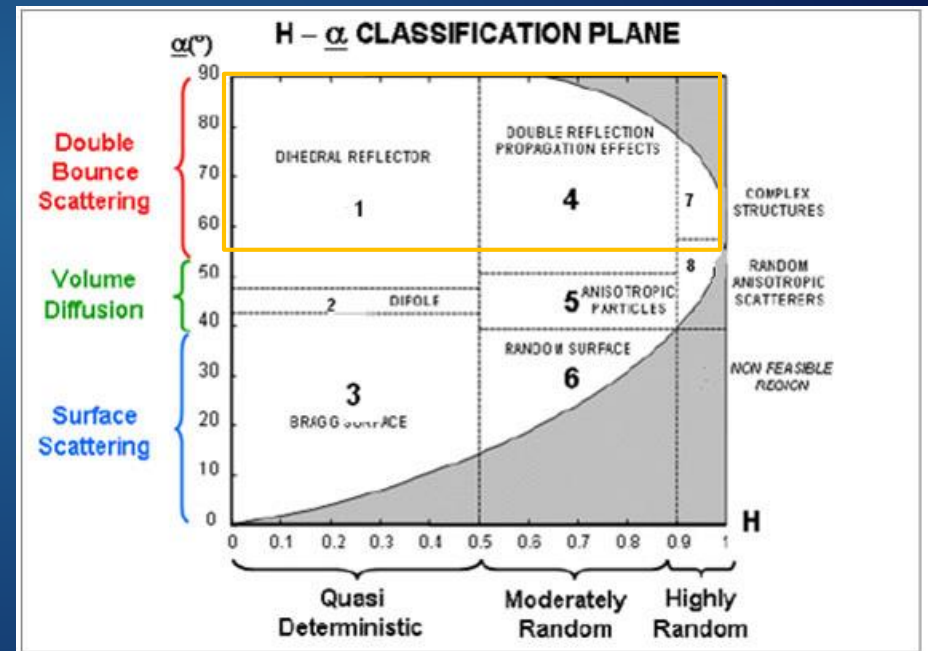
✓ Three parameters are derived [2]:

- **Entropy H** : measuring scattering degree of randomness.
- **Anisotropy A** : measuring the importance of second dominant mechanism.
- **Mean alpha α** : measuring the average scattering mechanism.

$$v_i = [\cos \alpha_i, \sin \alpha_i \cos \beta_i e^{i\delta_i}, \sin \alpha_i \sin \beta_i e^{i\gamma_i}]^T$$

$$H = \sum_{i=1}^3 \frac{\lambda_i}{\sum_{j=1}^3 \lambda_j} \log \left(\frac{\lambda_i}{\sum_{j=1}^3 \lambda_j} \right)$$

$$A = \frac{\lambda_2 - \lambda_3}{\lambda_2 + \lambda_3} \quad \alpha = \sum_{i=1}^3 \frac{\alpha_i \lambda_i}{\sum_{j=1}^3 \lambda_j}$$



[2] Cloude, S. R., and Pottier, E. "An Entropy Based Classification Scheme for Land Applications of Polarimetric SAR." *IEEE transactions on geoscience and remote sensing* 35.1 (1997): 68-78.

Temporal Wavelet Framework

- ✓ Let us consider a **signal temporal sequence** X_t for a fixed position (x, y) .
- ✓ L-taps **wavelet filter with response** W_b is applied on it.
- ✓ Two filters for **approximation** ($b = A$) and **detail** ($b = D$) **wavelet component** are considered.

Arithmetical Wavelet

- ✓ It is applied under the **assumption of additive Gaussian noise**.

$$X_{t-l}^{(Wab,k+1)}(x, y) = \sum_{l=0}^{L-1} W_b(l) X_{t-l}^{(WaA,k)}(x, y)$$

Geometrical Wavelet

- ✓ It is applied in presence of variables characterized by **multiplicative noise** [3].

$$X_{t-l}^{(Wgb,k+1)}(x, y) = \exp \left(\sum_{l=0}^{L-1} W_b(l) \log \left(X_{t-l}^{(WgA,k)}(x, y) \right) \right)$$

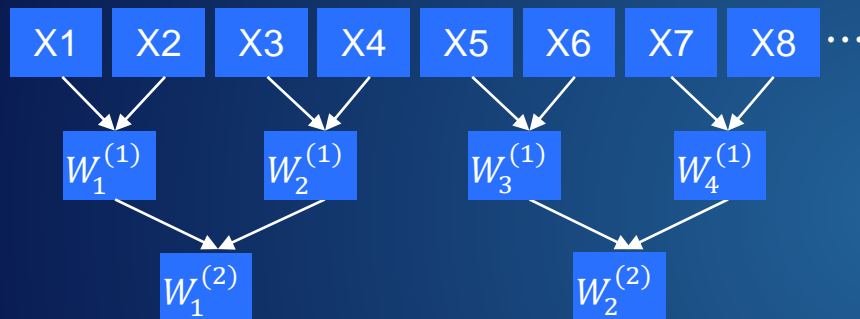
[3] Atto, A.M., et al. "Wavelet Operators and Multiplicative Observation Models—Application to SAR Image Time-series Analysis." *IEEE Transactions on Geoscience and Remote Sensing* 54.11 (2016): 6606-6624..

Wavelet Strategies

Without loss of generality, let us consider arithmetical wavelet on the time series.

Selection of **Haar wavelet family**, with coefficients $\frac{1}{\sqrt{2}} [1, 1]$ and $\frac{1}{\sqrt{2}} [1, -1]$.

Multi-scale DWT on two scale levels (MDW)

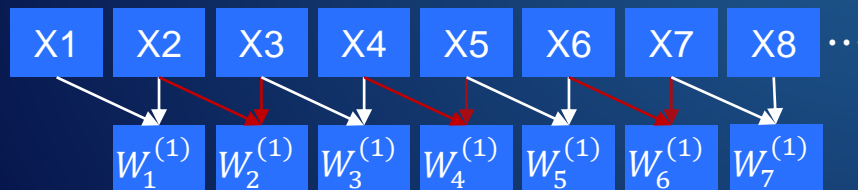


$$X_t^{(MDWa,k)} = \{X_t^{(MDWaA,k)}, X_t^{(MDWaD,k)}\}$$

$$X_t^{(MDWaA,k+1)} = \frac{1}{\sqrt{2}} (X_{t-1}^{(MDWaA,k)} + X_t^{(MDWaA,k)});$$

$$X_t^{(MDWaD,k+1)} = \frac{1}{\sqrt{2}} (X_{t-1}^{(MDWaA,k)} - X_t^{(MDWaA,k)});$$

Stationary wavelet on sequential pairs (SW)



$$X_t^{(SWa,1)} = \{X_t^{(SWaA,1)}, X_t^{(SWaD,1)}\}$$

$$X_t^{(SWaA,1)} = \frac{1}{\sqrt{2}} (X_{t-1} + X_t);$$

$$X_t^{(SWaD,1)} = \frac{1}{\sqrt{2}} (X_{t-1} - X_t);$$

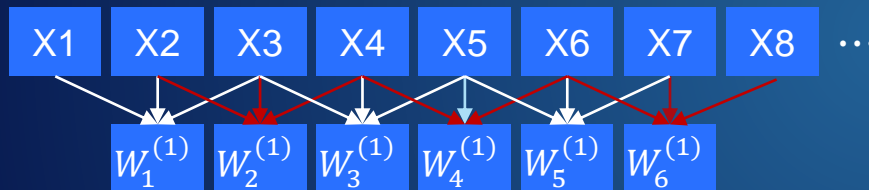
Difference (ratio) comparison operator equivalent to the Haar arithmetical (geometrical) temporal wavelet.

Wavelet Strategies

Let us assume the use of arithmetical wavelet on the time series.

Selection of **Haar wavelet family**, with coefficients $\frac{1}{\sqrt{2}} [1, 1]$ and $\frac{1}{\sqrt{2}} [1, -1]$.

Spline wavelet on sequential triplets (SSW)



$$X_t^{(SSWa,1)} = \{X_t^{(SSWaA,1)}, X_t^{(SSWaD,1)}\}$$

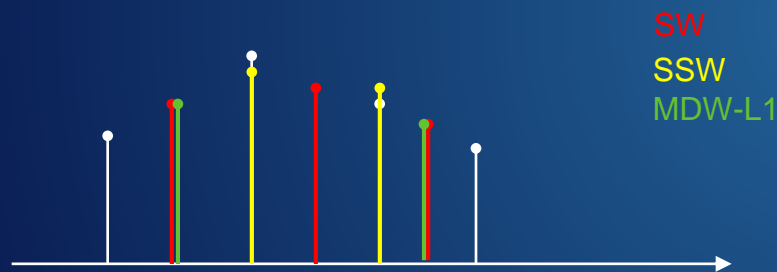
$$X_t^{(SSWaA,1)} = \frac{1}{\sqrt{6}} (X_{t-2} + 2X_{t-1} + X_t);$$

$$X_t^{(SSWaD,1)} = \frac{1}{\sqrt{6}} (X_{t-2} - 2X_{t-1} + X_t);$$

Approximation and Detail Components

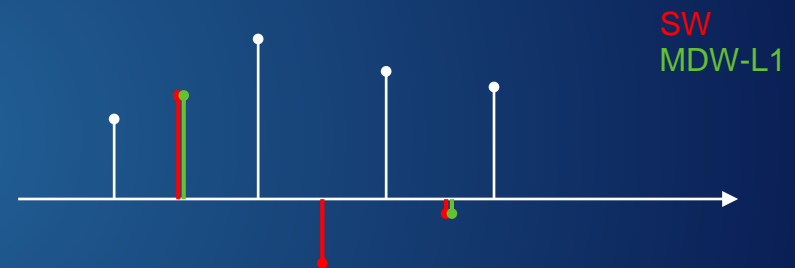
Approximation

- ✓ It can be used for a **robust separation of the classes** present in the image using the multi-temporal information.

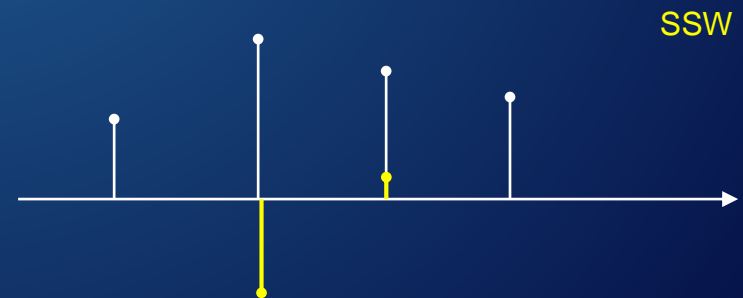


Detail

- ✓ It provides **information** about the **change in the feature**.
- ✓ For SW and MDW, the change is associated to a temporal variation.



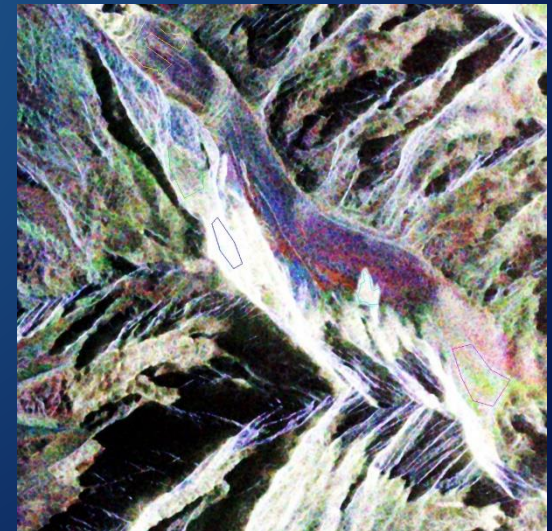
- ✓ For SSW the change is associated to a variation of the variation rate.



Experimental setup

Scene: Argentière glacier area (France)

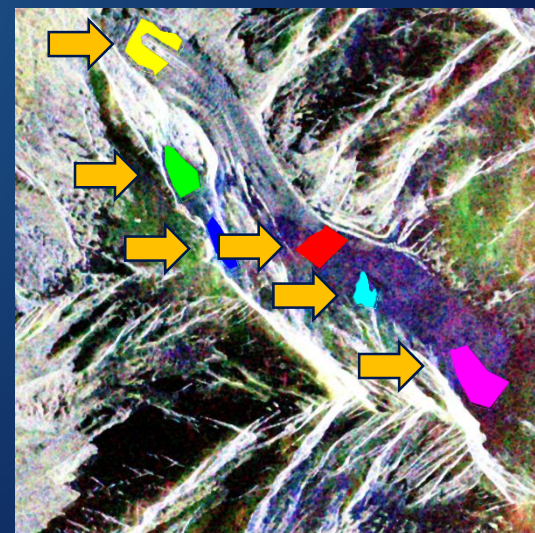
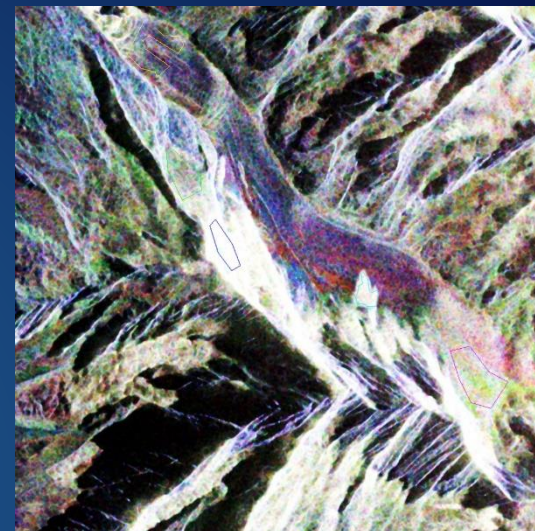
- ✓ 7 Multi-temporal Full-polarimetric SAR images from Radarsat-2 acquired in January-June, 2011
- ✓ Based on a preliminary similarity analysis with Gaussian and Gamma distribution, the wavelet selection led:
 - Arithmetical wavelet for CPD features;
 - Geometrical wavelet for Y4D features.
- ✓ Given the short temporal size of the time series, MDW strategy was not taken into account here.



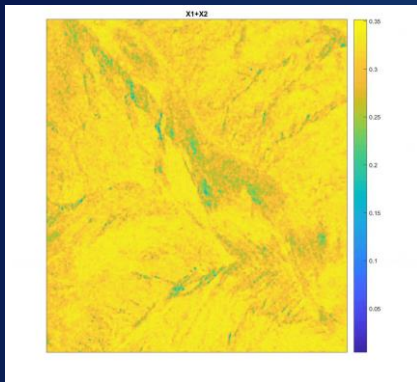
Experimental setup

Scene: Argentière glacier area (France)

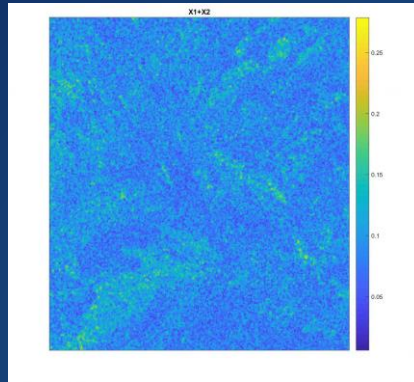
- ✓ 7 Multi-temporal Full-polarimetric SAR images from Radarsat-2 acquired in January-June, 2011
- ✓ Six regions of interest considered for local analysis.
 - Rognon glacier (north-south);
 - Ablation of Argentière (2400-2700m);
 - Avalanche area;
 - Accumulation area of the upper Argentière.



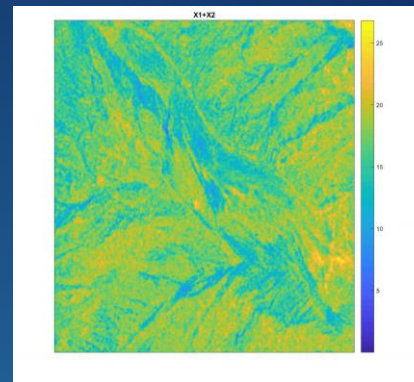
Experimental Results – SW Approximation



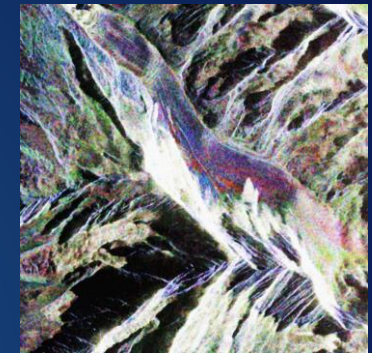
Entropy



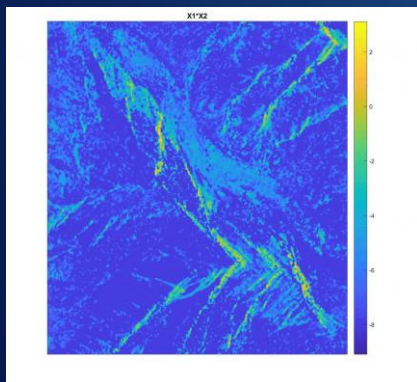
Anisotropy



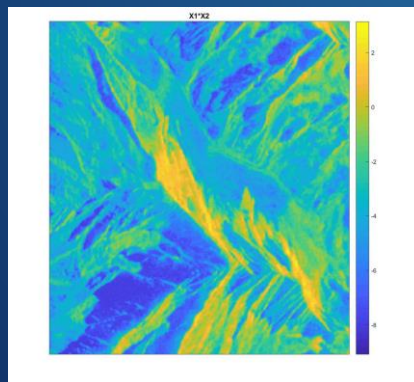
Alpha



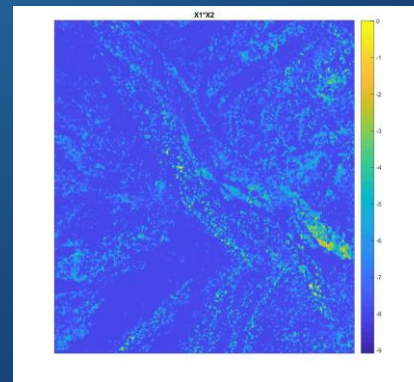
Pauli RGB



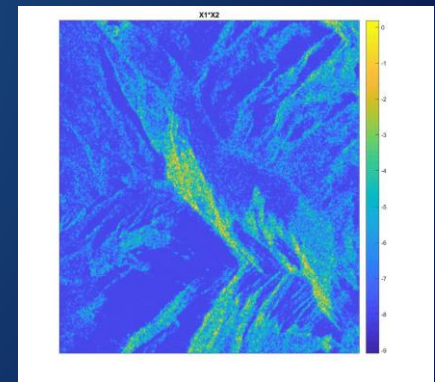
Surface



Volume

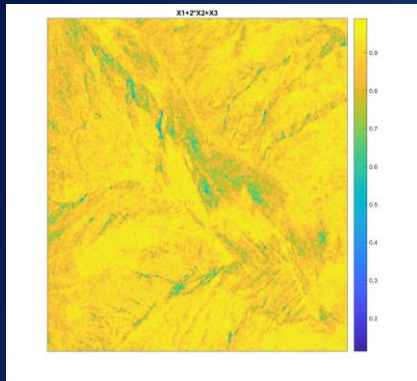


Double
Bounce

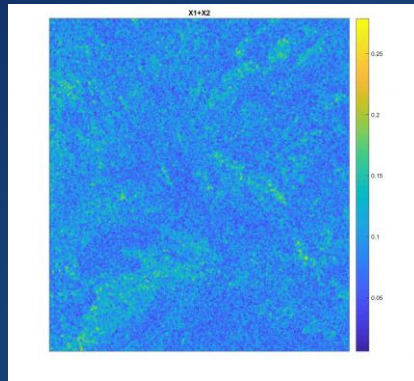


Helix

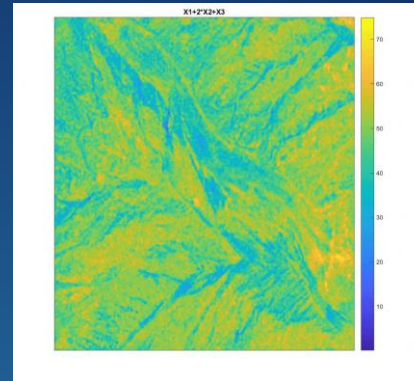
Experimental Results – SSW Approximation



Entropy



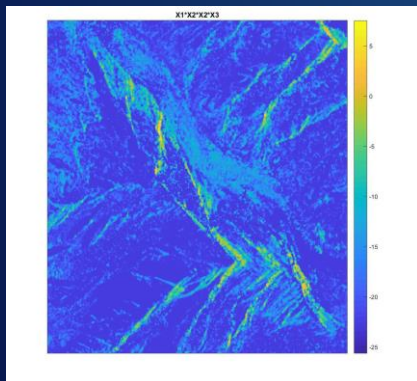
Anisotropy



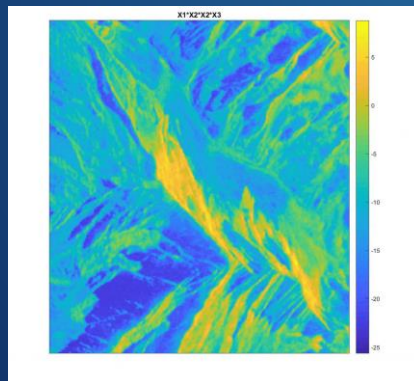
Alpha



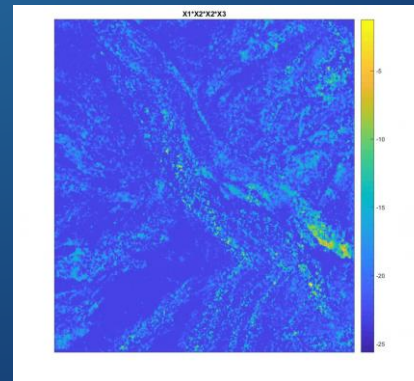
Pauli RGB



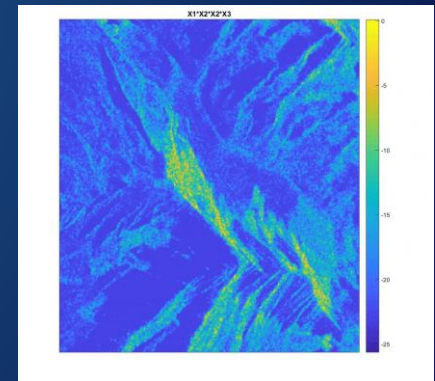
Surface



Volume

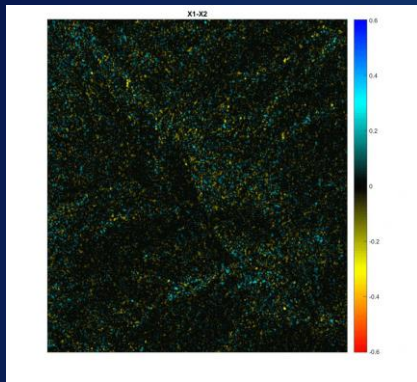


Double
Bounce

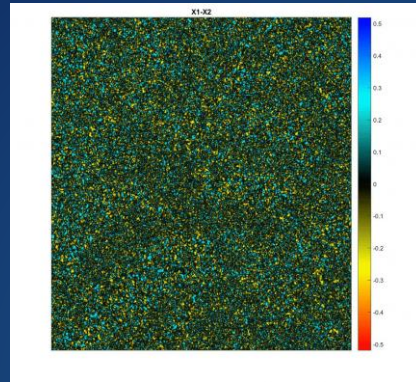


Helix

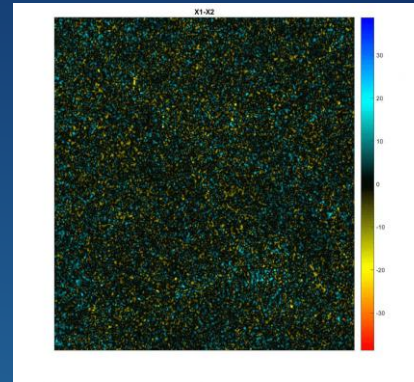
Experimental Results – SW Detail



Entropy



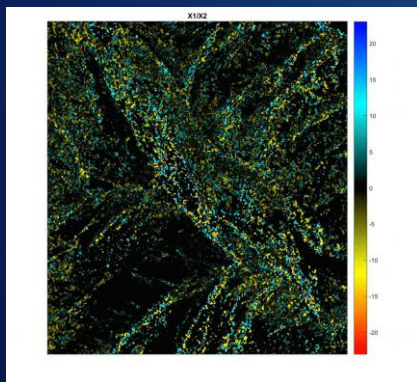
Anisotropy



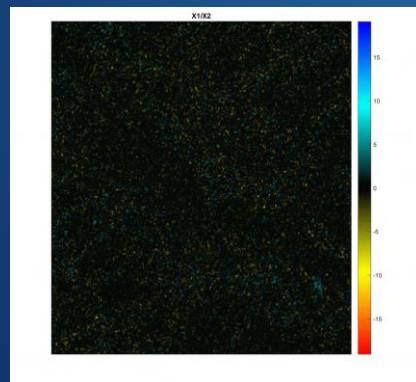
Alpha



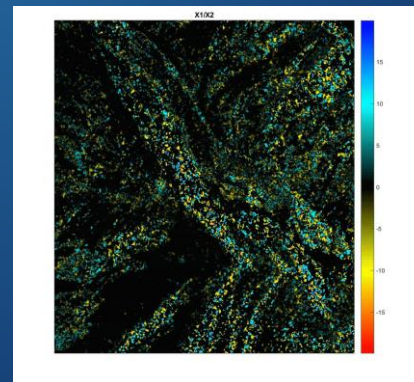
Pauli RGB



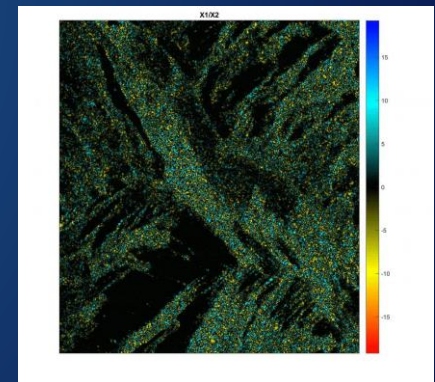
Surface



Volume

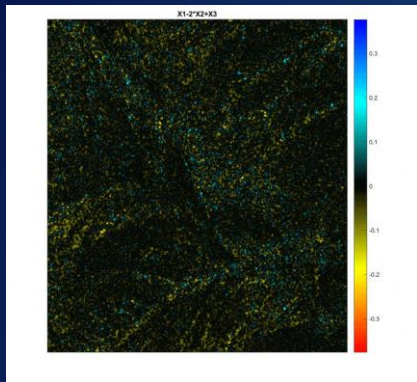


Double
Bounce

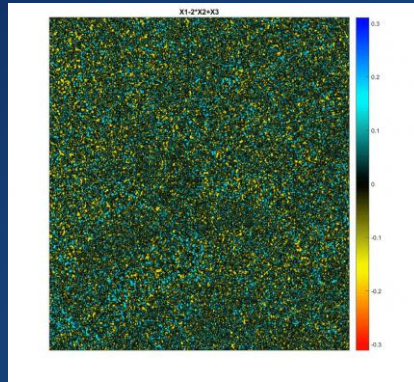


Helix

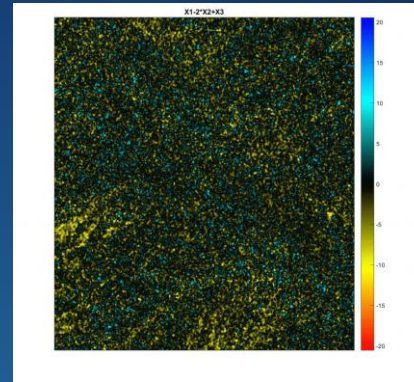
Experimental Results – SSW Detail



Entropy



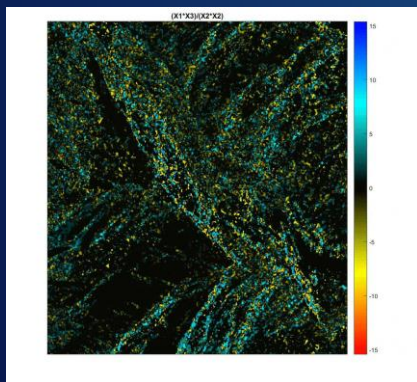
Anisotropy



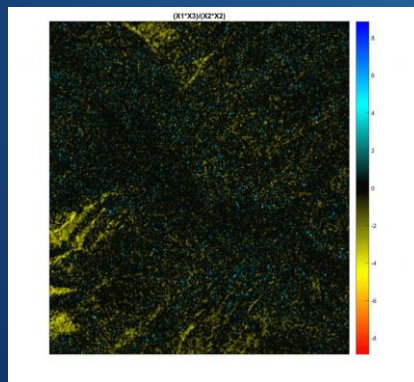
Alpha



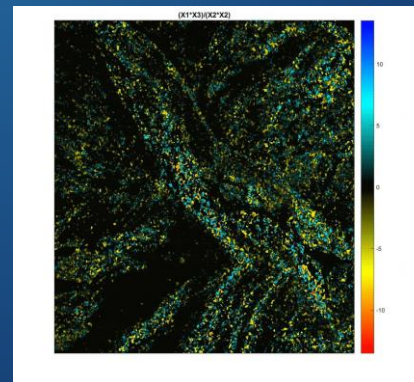
Pauli RGB



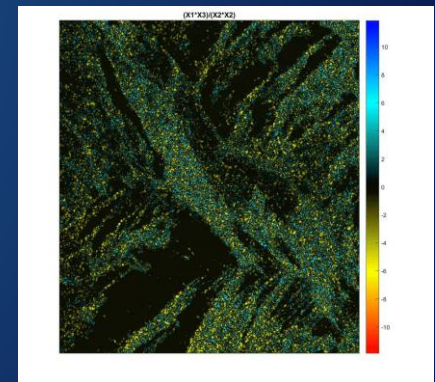
Surface



Volume

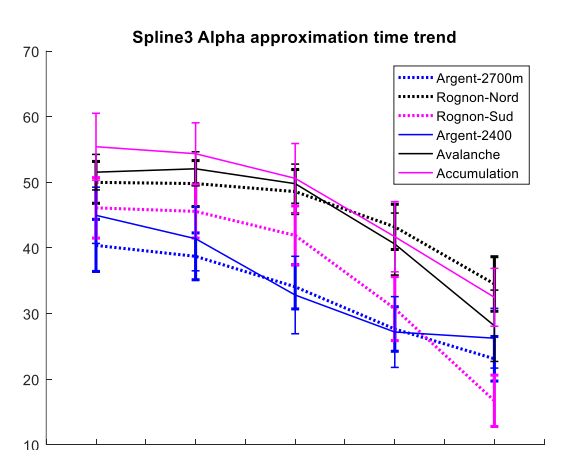
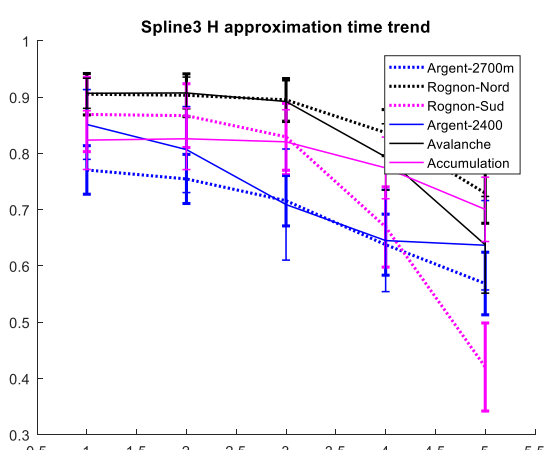
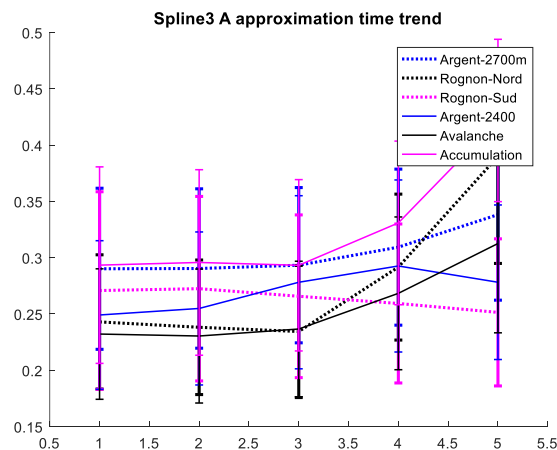
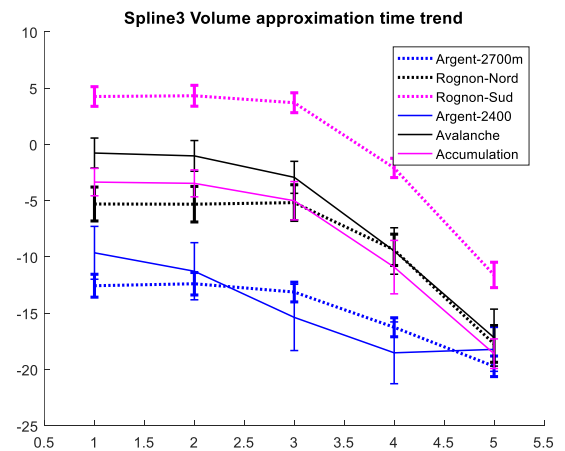
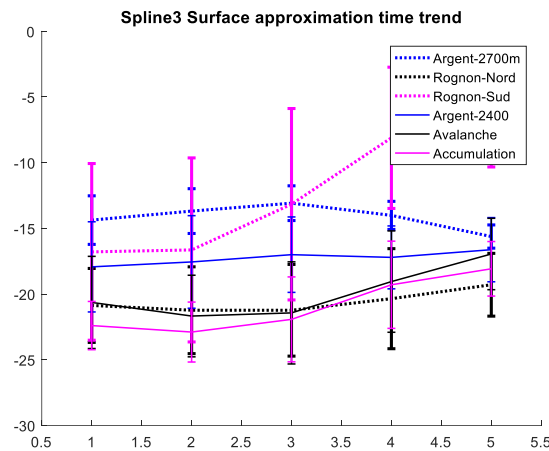
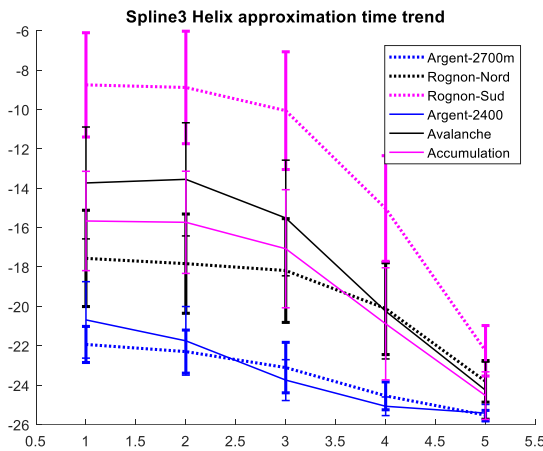


Double
Bounce

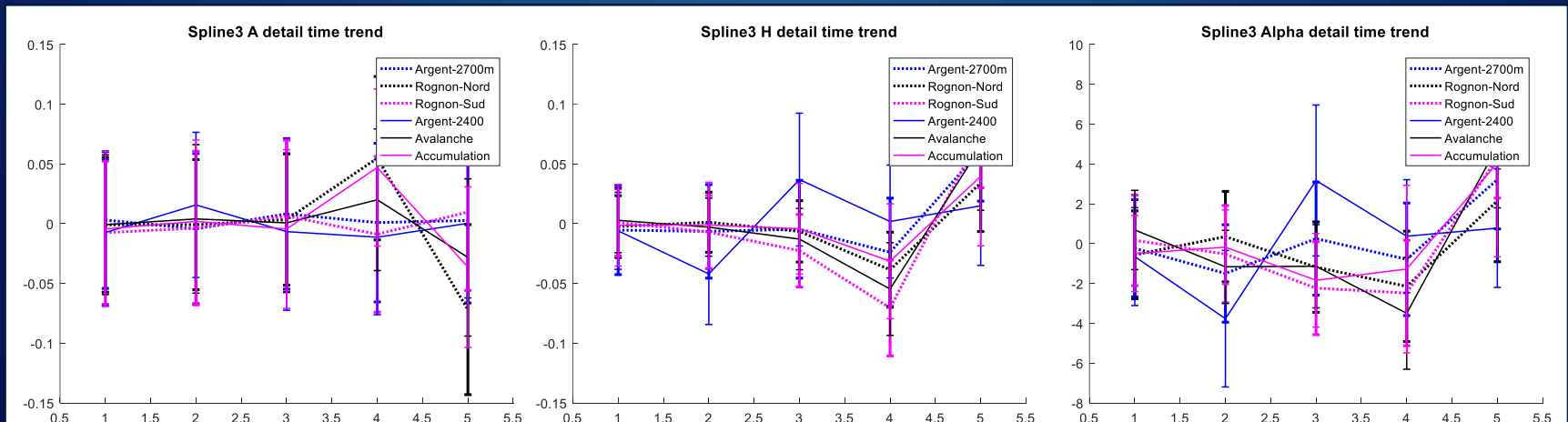
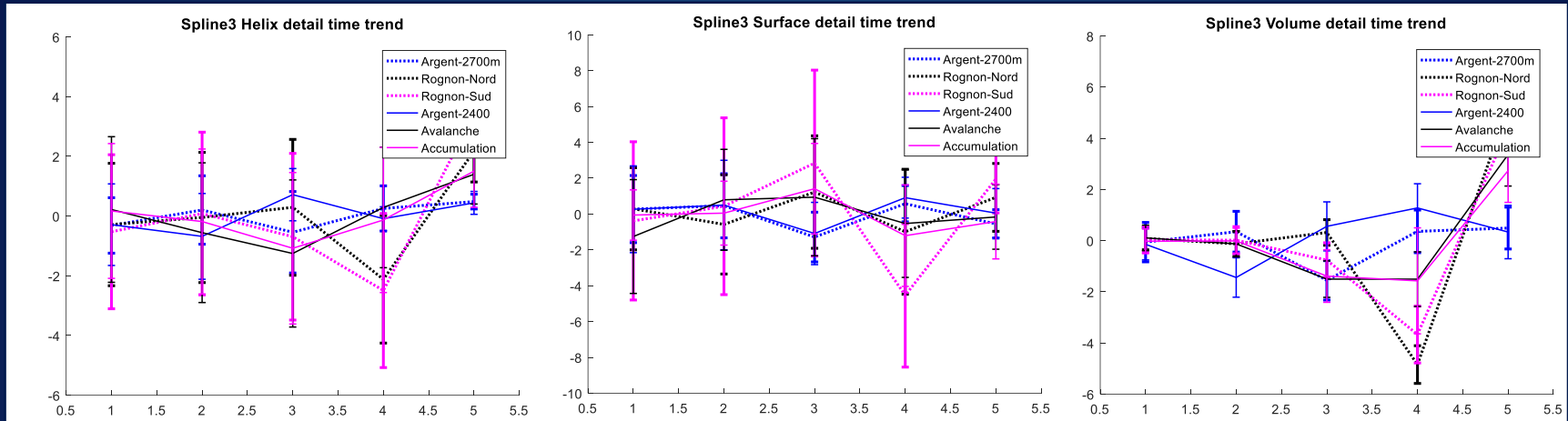


Helix

Experimental results – Local Analysis



Experimental results – Local Analysis



Time-series Spatio-temporal Descriptors

Approximation

- ✓ It can be used for a **robust separation of the classes** present in the image using the multi-temporal information.
- ✓ An **Overall Class Separation Indicator (OCSI)** is defined for measuring the global **effectiveness of the class separation**.

$$OCSI(w, X) = \sum_{c1} \sum_{c2 \neq c1} \sum_t \frac{|\mu_{wXt}^{(c1)} - \mu_{wXt}^{(c2)}|}{\sqrt{(\sigma_{wXt}^{(c1)})^2 + (\sigma_{wXt}^{(c2)})^2}}$$

Detail

- ✓ It provides **information about the change or the change velocity**.
- ✓ Two indices are defined:
 - **Change Rate R_C** , describing the smoothness degree;
 - **dynamicity index δ** , describing the **overall change** in the time series.

$$\delta(w, X) = \sum_c \sum_t \frac{|\mu_{wXt}^{(c1)}|}{(\sigma_{wXt}^{(c1)})}$$

$$R_C(w, X) = \sum_c \left[\max_t \left(\frac{|\mu_{wXt}^{(c1)}|}{(\sigma_{wXt}^{(c1)})} \right) / \sum_t \frac{|\mu_{wXt}^{(c1)}|}{(\sigma_{wXt}^{(c1)})} \right]$$

Experimental results – Local Analysis

Overall Class Separation Indicator	SW	SSW	MDW
H	101.1425	87.7184	67.0577
A	37.3631	30.8456	25.4238
α	115.5167	102.6236	74.0808
Aggregate (Eigen-based)	84.6741	73.7292	55.5208
f_d	24.0888	20.5587	15.1726
f_h	114.4109	122.2092	68.6441
f_s	30.5785	78.1185	62.2078
f_v	284.6874	253.6868	171.4954
Aggregate (Power-based)	129.4414	118.6433	79.38

Experimental results – Local Analysis

Dynamicity	SW	SSW	MDW
H	3.4835	2.7232	2.2891
A	1.1174	0.9527	0.7635
α	4.4582	3.0593	2.7089
Aggregate (Eigen-based)	3.0197	2.2451	1.9205
f_d	2.2224	1.4850	1.2574
f_h	8.0742	5.1397	3.8863
f_s	2.4793	1.8746	0.7537
f_v	7.2983	6.9903	4.7206
Aggregate (Power-based)	5.0186	3.8724	2.6545

Change Rate	SW	SSW	MDW
H	0.5976	0.4709	0.8755
A	0.4974	0.4359	0.7167
α	0.4663	0.4210	0.7601
Aggregate (Eigen-based)	0.5204	0.4426	0.7841
f_d	0.3917	0.5709	0.6901
f_h	0.5546	0.6227	0.8994
f_s	0.3930	0.3824	0.5540
f_v	0.5784	0.4855	0.8752
Aggregate (Power-based)	0.4794	0.5154	0.7547

Conclusions and Future Developments

Conclusions

- ✓ We presented a novel framework based on temporal wavelet transform for analysis of polarimetric image time series.
- ✓ The framework considered different wavelet strategies and polarimetric features for discriminating both different temporal evolution on the changes and multi-temporal classes.
- ✓ A sensitivity analysis on the features was conducted for looking at those more sensitive to temporal changes.
- ✓ Experimental results in glacier evolution scenario showed the effectiveness of the proposed framework in separating classes and tracking change evolution.

Future Developments

- ✓ Integrating the framework with a unsupervised/supervised CD strategy.
- ✓ Combining features from the application of different wavelet families.
- ✓ Exploiting wavelet decomposition in both spatial and temporal domain.